Parametric study of optical forces acting upon nanoparticles in a single, or a standing, evanescent wave

2011 J. Opt. 13 044016

(http://iopscience.iop.org/2040-8986/13/4/044016)

IOP Publishing Journal of Optics
J. Opt. **13** (2011) 044016 (9pp) doi:10.1088/2040-8978/13/4/044016

Parametric study of optical forces acting upon nanoparticles in a single, or a standing, evanescent wave

Martin Šiler and Pavel Zemánek

Institute of Scientific Instruments of the ASCR v.v.i., Academy of Sciences of the Czech Republic, Královopolská 147, 612 64 Brno, Czech Republic

E-mail: siler@isibrno.cz and zemanek@isibrno.cz

Received 17 May 2010, accepted for publication 6 September 2010
Published 4 March 2011
Online at stacks.iop.org/JOpt/13/044016

Abstract
We compare four different methods for calculating the optical forces acting upon nanoparticles illuminated either by a single evanescent wave or by an interference field of two counter-propagating coherent evanescent waves (standing evanescent wave). Two of the employed methods consider the effect of multiple reflections of the scattered field from the water–prism interface that generates the illuminating evanescent wave(s). Subsequently, we present a parametric study of the optical forces acting upon nanoparticles for different polarizations and propagation constants of the illuminating evanescent wave, particle sizes and refractive indices.

Keywords: optical tweezers, optical lattice, optical force, evanescent wave

(Some figures in this article are in colour only in the electronic version)

1. Introduction

An evanescent wave (or near-field) describes an electromagnetic field that does not propagate in space at least in one direction and exists only in the close vicinity of material interfaces or sub-wavelength-sized structures. Such a non-propagating nature in some directions is caused by the pure imaginary part of the corresponding evanescent wave wavevector. Therefore, the evanescent wave intensity decays exponentially along these directions and the interaction of the evanescent wave (EW) with external objects is limited to a proximity of the EW source, i.e. to a region smaller than the light wavelength. Such a spatial reduction of the illuminated region has been utilized in new techniques of optical microscopy—total internal reflection fluorescence microscopy (TIRFM) [1] and near-field scanning optical microscopes [2–4] that offer a higher spatial resolution than conventional microscopy techniques exploiting the propagating (far-field or radiative) fields.

The classical method of evanescent field generation uses the total internal reflection of light at a dielectric interface between a glass prism and a medium having lower refractive index (so-called Kretschmann configuration). If a suspension of microparticles is placed on the prism surface, the EW penetrates into it and influences the motion of the dispersed particles (see figure 1). In early 1990s Kawata *et al* proved that the EW can indeed serve as an alternative configuration for the optical manipulation of micro-objects on a surface [5].

Optical micromanipulation methods use the transfer of momentum from light to micron and submicron-sized objects and such interaction forms the so-called optical force. The most frequent configurations for confining small objects in space employ a single tightly focused Gaussian beam (so-called optical tweezers) [6] or counter-propagating wider Gaussian beams (dual-beam trap) [7]. In the last 40 years both configurations have been developed and found numerous applications in physics, chemistry, engineering and biology [8–12]. In contrast to optical tweezers and dual-beam traps, a setup using the EW does not need focusing optics to manipulate objects and, therefore, it is sometimes called lens-free. Moreover, it also provides more flexibility in the design, such as a varying number of incident laser beams and a much larger illuminated area over which the particles can be manipulated or organized [13–19]. However, the disadvantage is usually a more complex and less stable setup.

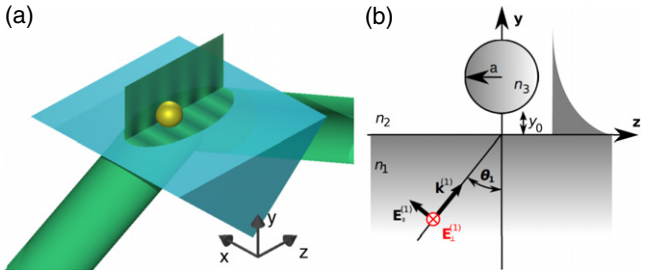

Figure 1. Schematic depiction of the studied configuration. Quantity y_0 denotes the separation of the particle from the prism surface; the other symbols are explained in the text.

From the theoretical point of view, the calculation of the optical forces acting upon a particle illuminated by the EW is tightly connected to the determination of the spatial distribution of the total electromagnetic field around the particle. This field is obtained by the interference of the illuminating EW with the field scattered by the particle and by other involved surfaces/interfaces. The theoretical descriptions of such a total field have been developed especially for the purposes of near-field microscopy [20, 21]. Several studies described theoretically the optical forces acting upon a spherical particle in the EW using various approaches and levels of complexity. The majority of them considered the EW scattered by the particle and ignored the total field modification caused by multiple scattering between the particle and the surface [13, 22–37]. Just a few studies considered the influence of the surface on the total interaction between the illuminating EW and the particle and, consequently, on the optical forces acting upon the particle [29, 31, 38–42]. In this paper, we first compare four different methods (namely, Rayleigh approximation, Rayleigh approximation with correction to the dielectric interface proximity, Mie scattering, and the finite element method) for calculating the optical forces acting upon a sub-wavelength-sized particle illuminated by the EW. Two of the considered methods include the influence of a planar dielectric interface on the resulting optical force. We evaluate the performance of these methods and the error introduced into the calculations for different distances of the particle from the dielectric interface. In the second part, we present a parametric study of the optical forces acting upon a particle placed in a single EW or in counter-propagating interfering EWs (forming an evanescent standing wave along the surface with an exponential decease of its amplitude away from the surface) for different polarizations and propagation constants of the illuminating evanescent wave, particle sizes, and refractive indices. All the theoretical results presented here use a polystyrene particle of refractive index $n_3 = 1.59$ placed in water ($n_2 = 1.334$) and in the proximity of a BK7 glass prism ($n_1 = 1.519\,47$). The vacuum wavelength of the trapping light is $\lambda_{\mathrm{vac}} = 532$ nm and its electric field intensity is equal to $|\mathbf{E}_0^{(1)}| = 1.9 \times 10^7$ V m^{-1}. This corresponds to the electric field intensity in the centre of the Gaussian beam waist if the laser power is $P = 1$ W and the waist radius is $w_0 = 1$ μm. The typical experimentally achieved values are approximately 10–100× lower; however, the optical forces are directly proportional to the laser power and thus the actual forces can be easily rescaled.

2. Description of the evanescent wavefield

Let us consider a plane wave impinging on a planar interface between two media characterized by refractive indices n_1 (prism) and n_2 (water) (see figure 1).

If $n_2 < n_1 \sin\theta_1$, where θ_1 is the angle of a plane wave incidence at the interface, Snell's law $n_1 \sin\theta_1 = n_2 \sin\theta_2$ can be fulfilled only if the angle of refraction θ_2 is imaginary and, therefore, the refracted (transmitted) wave becomes the evanescent wave. The so-called critical incident angle θ_{c} fulfils $n_2 = n_1 \sin\theta_{\mathrm{c}}$ and it leads to a transmitted wave propagating along the surface. For the above mentioned values of the refractive indices we obtain the value of the critical angle $\theta_{\mathrm{c}} = 61.395°$. If the angle of incidence is larger than the critical angle, the evanescent wave propagates similarly along the surface (i.e. along **z** direction in figure 1) but its amplitude exponentially decays into the medium with a refractive index n_2 (i.e. along **y** direction in figure 1).

An arbitrarily polarized incident plane wave $\mathbf{E}_0^{(1)} \exp(\mathrm{i}\mathbf{k}_1\mathbf{r} - \mathrm{i}\omega t)$ can be described as the superposition of two orthogonally polarized plane waves with their polarizations parallel ($E_{\parallel}^{(1)}$, often called a p-polarized or TM-polarized wave) or perpendicular ($E_{\perp}^{(1)}$, s-polarized or TE-polarized wave) to the plane of incidence. Following the coordinates and geometry from figure 1, the electric field $\mathbf{E}^{(2)}$ at an arbitrary place above the interface can be expressed in terms of the unit vectors **x**, **y**, **z** as follows (the time dependent factor $-\mathrm{i}\omega t$ is omitted)

$$\mathbf{E}^{(2)} = (\mathbf{x}E_{\perp}^{(2)} + \mathbf{y}E_{\parallel}^{(2)} \sin\theta_2 - \mathbf{z}E_{\parallel}^{(2)} \cos\theta_2) \exp(\mathrm{i}\mathbf{k_2}\mathbf{r}). \quad (1)$$

The intensities $E_{\perp}^{(2)}$ and $E_{\parallel}^{(2)}$ are given by the Fresnel coefficients of transmission $T_{\parallel}$ and $T_{\perp}$ as follows

$$\begin{aligned} E_{\perp}^{(2)} &= T_{\perp}E_{\perp}^{(1)} = \frac{2\cos\theta_1}{\cos\theta_1 + \mathrm{i}\sqrt{\sin^2\theta_1 - n_{21}^2}} E_{\perp}^{(1)}, \\ E_{\parallel}^{(2)} &= T_{\parallel}E_{\parallel}^{(1)} = \frac{2n_{21}\cos\theta_1}{n_{21}^2\cos\theta_1 + \mathrm{i}\sqrt{\sin^2\theta_1 - n_{21}^2}} E_{\parallel}^{(1)}, \end{aligned} \quad (2)$$

where n_{21} is the ratio of the refractive index of the liquid and the prism ($n_{21} = n_2/n_1$) and θ_1 is expected to be larger than the critical angle θ_{c}. The optical forces are expressed in the Cartesian system of coordinates introduced in figure 1 and, therefore, the electric field at an arbitrary point above the interface can be rewritten as

$$\mathbf{E}^{(2)} = \left(\mathbf{x}E_x^{(2)} + \mathbf{y}E_y^{(2)} + \mathbf{z}E_z^{(2)}\right) \exp\left(-\beta y + \mathrm{i}\gamma z\right), \quad (3)$$

where

$$\begin{aligned} E_x^{(2)} &= T_{\perp}E_{\perp}^{(1)}, \quad E_y^{(2)} = \frac{1}{n_{21}} T_{\parallel}E_{\parallel}^{(1)} \sin\theta_1, \\ E_z^{(2)} &= -\frac{\mathrm{i}}{n_{21}} T_{\parallel}E_{\parallel}^{(1)} \sqrt{\sin^2\theta_1 - n_{21}^2}, \\ \beta &= \frac{2\pi n_1}{\lambda_{\mathrm{vac}}} \sqrt{\sin^2\theta_1 - n_{21}^2}, \qquad \gamma = \frac{2\pi n_1}{\lambda_{\mathrm{vac}}} \sin\theta_1. \end{aligned} \quad (4)$$

The factor β denotes the damping factor of the electric field intensity above the prism and γ corresponds to the wavenumber of the evanescent wave propagating along the **z** direction.

3. Optical forces in an evanescent field near a dielectric interface: a comparison of different computation approaches

Let us first deal with the simplest possible experimental configuration, similar to the original work of Kawata [5], where the EW is created by a single incident plane wave and a single particle is propelled due to the EW above the prism. In the following comparison we consider a single polystyrene particle of two different radii $a = 5$ and 50 nm.

3.1. Rayleigh approximation (RA)

This approximation is generally accepted for the calculation of the time averaged optical forces acting upon nanoparticles with radii smaller than $\sim\lambda/20$. Its biggest advantage is that it provides the analytical expression for such forces [43, 44]:

$$F_\xi = \frac{1}{2}\Re\left\{\sum_{\zeta=x,y,z}\alpha E_\zeta \frac{\partial E_\zeta^*}{\partial \xi}\right\}, \qquad \xi = x, y \text{ or } z, \tag{5}$$

where X^* and $\Re(X)$ denote a complex conjugated value and a real value of X, respectively. The particle polarizability α is expressed as [45]

$$\alpha = \frac{\alpha_0}{1-\frac{\mathrm{i}k_2^3\alpha_0}{6\pi\varepsilon_2\varepsilon_0}}, \qquad \text{where } \alpha_0 = 4\pi a^3\varepsilon_2\varepsilon_0\frac{n_{32}^2-1}{n_{32}^2+2} \tag{6}$$

and $n_{32} = n_3/n_2$.

If we consider the illuminating EW in the form of equation (3), the resulting force acting upon a particle is expressed as [16]

$$\mathbf{F} = \tfrac{1}{2}\Re\{\alpha(\mathbf{x}F_{0x} + \mathbf{y}F_{0y} + \mathbf{z}F_{0z})\exp(-2\beta y)\}, \tag{7}$$

where $F_{0x} = 0$ and

$$\begin{aligned} F_{0y} &= -\beta|T_\perp|^2E_\perp^{(1)2} - \frac{\beta}{n_{21}^2}|T_\parallel|^2E_\parallel^{(1)2}(2\sin\theta_1 - n_{21}^2),\\ F_{0z} &= -\mathrm{i}\gamma|T_\perp|^2E_\perp^{(1)2} - \frac{\mathrm{i}\gamma}{n_{21}^2}|T_\parallel|^2E_\parallel^{(1)2}(2\sin\theta_1 - n_{21}^2). \end{aligned} \tag{8}$$

3.2. Rayleigh approximation with correction to the surface (RASC)

The effect of multiple reflections of the scattered light between the Rayleigh particle and the interface is incorporated similarly as in [39]. If the optical force is expressed using equation (7), the coefficients F_{0y} and F_{0z} are given as follows:

$$\begin{aligned} F_{0y} &= -\beta\left(\frac{|E_{0x}|^2+|E_{0z}|^2}{1+\frac{\alpha\Delta}{8\varepsilon_2\varepsilon_0y^3}} + \frac{|E_{0y}|^2}{1+\frac{\alpha\Delta}{4\varepsilon_2\varepsilon_0y^3}}\right)\\ &\quad + \frac{3\alpha^*\Delta}{16y^4}\left(\frac{|E_{0x}|^2+|E_{0z}|^2}{|1+\frac{\alpha\Delta}{8\varepsilon_2\varepsilon_0y^3}|^2} + \frac{2|E_{0y}|^2}{|1+\frac{\alpha\Delta}{4\varepsilon_2\varepsilon_0y^3}|^2}\right),\\ F_{0z} &= -\mathrm{i}\gamma\left(\frac{|E_{0x}|^2+|E_{0z}|^2}{1+\frac{\alpha\Delta}{8\varepsilon_2\varepsilon_0y^3}} + \frac{|E_{0y}|^2}{1+\frac{\alpha\Delta}{4\varepsilon_2\varepsilon_0y^3}}\right), \end{aligned} \tag{9}$$

where y denotes the distance of the particle centre from the prism surface, $\Delta = (n_2^2-n_1^2)/(n_2^2+n_1^2)$ is the Fresnel reflection coefficient of the surface in the case of normal incidence, and the electric field intensities E_{0x}, E_{0y} and E_{0z} are given by the equations (1) and (4), i.e. $E_{0x} = E_x^{(2)}\exp(-\beta y + \mathrm{i}\gamma z)$ and similarly for E_{0y} and E_{0z}.

3.3. Mie scattering based method (MSM)

The MSM represents the most efficient way of calculating the optical force acting upon a single larger spherical particle far from any additional material interfaces [14, 16, 22, 23, 46–48]. In general, multiple reflections of the scattered field between the interface and the particle can be incorporated using the spectrum of plane waves [21, 38, 49]. However, this approach is more computationally demanding and it is not used in this paper. The description of the force interaction between a light wave and a particle is based on the momentum conservation principle: forces acting on any finite volume in a material body can be expressed through the forces applied to the surface of that volume. Furthermore, we assume that the fluid surrounding the particle is isotropic, non-magnetic, linear in its response to the applied field, and in hydrodynamic equilibrium. In this case, the time averaged total electromagnetic force acting upon the particle is equal to the integral of the dot product of the outward directed unit normal vector **n** and the Maxwell's stress tensor in Minkowski form $\mathbf{T}^{\mathrm{M}}$ over an arbitrary surface S enclosing the particle [46, 50]:

$$\langle F_i\rangle = \left\langle \oint_S \sum_j T_{ij}^{\mathrm{M}} n_j \,\mathrm{d}S\right\rangle, \tag{10}$$

$$T_{ij}^{\mathrm{M}} = [\varepsilon E_iE_j + \mu_0H_iH_j - \tfrac{1}{2}(\varepsilon E^2 + \mu_0H^2)\delta_{ij}], \tag{11}$$

where ε is the permittivity of the surrounding medium and μ_0 is the permeability of vacuum. The components of the vectors of the electric and magnetic intensity E_i and H_i have to be obtained as the sums of the incident and scattered fields. In this work, we adapted the algorithm described by Almaas [23] and applied it in the case of a single illuminating EW and two counter-propagating EWs [16].

3.4. Finite element method calculations (FEM)

The FEM discretizes the volume containing the considered material bodies into sufficiently small volume elements and applies numerical methods to solve Maxwell's equations with appropriate boundary conditions. In principle, FEM provides the total fields surrounding a particle of any shape taking into

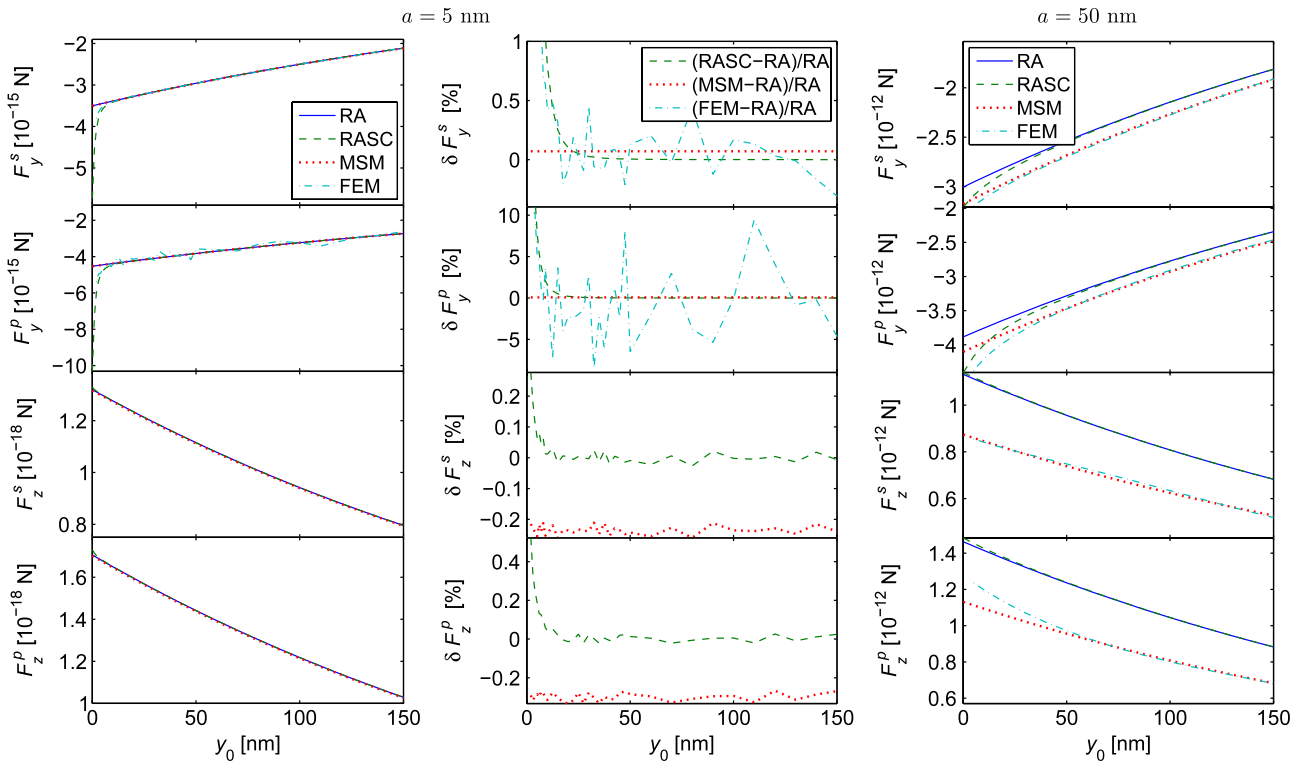

Figure 2. The comparison of the optical forces calculated by all four presented methods (FEM, MSM, RA, and RASC). Particles of radii 5 nm and 50 nm (left and right column, respectively) are considered. The components of the total force in the **y** and **z** directions (F_y^s, F_y^p, F_z^s and F_z^p) are shown as functions of the particle—surface separation y_0 for both s- and p-polarizations of the incident plane wave forming the EW. Because of large numerical error the forces F_z^s and F_z^p obtained from the FEM calculations for the smaller particle with radius $a = 5$ nm are not shown. The central column shows the relative difference between optical forces calculated by RA and the other three methods for the smaller particle ($a = 5$ nm).

account the presence of an additional dielectric interface. If the obtained fields are used in equation (11), the optical force acting upon the particle can be determined [31].

We calculated the scattered field around a sphere placed above a dielectric interface using the COMSOL Multiphysics package. The considered geometry covered the particle, its surrounding volume, and a part of the prism volume as well. We employed the mirror symmetry of the studied problem along the plane of incidence in order to decrease the number of elements and lower the computational demands. Despite these steps, we were still limited by the PC memory and we could only handle particles of radii up to $\sim\lambda/4$. Upon calculating the total field surrounding the particle, equations (10) and (11) were used to calculate the optical force. The value of the obtained optical force must not depend on the surface S chosen for integration in equation (10). In order to verify the consistency of our results, we calculated the final force by integrating equation (10) over spheres of a varying radius b. In particular, we considered three values of b that were larger than the particle radius a by 2, 5, and 10 nm. We found differences between F_y values within 1% due to the different meshing of the studied volume. However, if the force F_z is much smaller than F_y, the order of magnitude of F_z reaches the level of numerical errors presented in FEM calculations and, thus, we obtain unreliable values of F_z.

3.5. Discussion

The results of all four methods are compared in figure 2. The optical forces calculated for the smallest particle of radius 5 nm coincide very well for all methods. Both methods considering the influence of the interface (i.e. FEM and RASC) give very similar results for F_y if the particle is closer to the interface. All four methods give similar results for F_y if the particle is farther from the interface. The influence of the numerical errors is visible in F_y^p calculated by FEM. The force F_z is three orders of magnitude weaker than F_y and, consequently, it becomes of the same order of magnitude as the numerical errors presented in the FEM calculations. Therefore, the FEM results of F_z are not presented for this particle size.

Considering the bigger particle, significant differences are visible between the RA and RASC approaches compared to FEM and MSM. FEM and MSM give similar results if the particle is farther from the interface, however, as the particle approaches the interface, the optical forces obtained by both approaches start to differ. This trend is more significant for a p-polarized incident plane wave. Figure 3 considers a particle of radius 50 nm and shows the relative differences of the optical forces calculated by FEM and MSM for both s and p-polarized incident plane waves. This relative difference is higher near the interface but it is still less than 8%. Farther from the interface the relative difference displays oscillations with the period

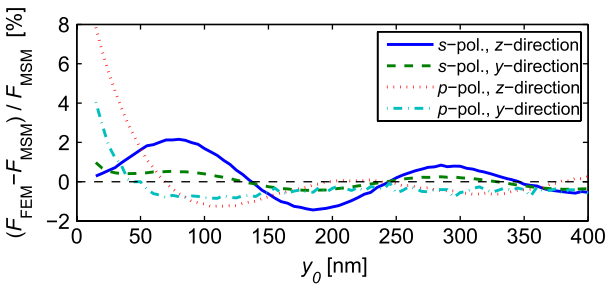

Figure 3. Relative differences between the optical forces acting upon the particle of radius 50 nm calculated by FEM and MSM.

length close to 200 nm. These oscillations correspond to a standing wave created by the interference of the light scattered by the particle and retro-reflected scattered light because the wavelength of the considered light in water is close to 400 nm.

4. Parametric studies

The previous section showed that if the particle is not in the vicinity of the interface, the MSM provides reasonable information about the forces acting upon the particle. Since MSM is several orders of magnitude faster than FEM and it is not limited by the computer memory, we use MSM to perform parametric studies of the optical forces in the evanescent wave as the first-order approximation. It has been shown [16, 23] that the optical forces decay exponentially as $\exp(-2\beta y_0)$. Therefore, if we neglect the interface influence studied above, we can assume that the particle is in contact with the surface because the results can be easily transformed to different particle–surface separations.

4.1. Single incident plane wave

First we focus on the forces F_y and F_z and their dependences on the plane wave incidence angles θ_1 on the prism and particle diameter $d = 2a$. The results for s- and p-polarized incident plane waves are shown in figure 4. The angles of incidence $\theta_1 > 70°$ are not considered because in this angular range the forces decay fast to zero and do not influence the particle motion.

Figure 5 shows the dependence of the forces F_y and F_z on the particle diameter and the particle refractive index n_3 in the range from 1 up to 2. This selection of refractive indices covers both particles of refractive indices higher and lower compared to the surrounding medium with $n_2 = 1.33$. Therefore, the force F_y changes its sign because particles of a lower refractive index are repelled from the regions of high optical intensity, i.e. away from the interface.

The results in figures 4 and 5 lead to the following conclusions and comments:

- If the particle refractive index n_3 is larger (smaller) than the refractive index of the ambient medium n_2, the optical forces attract (repel) the particle towards (away from) the interface (in the **y** direction). The optical forces also get stronger with an increasing difference between the medium and the particle refractive index. Furthermore, the optical forces push the particle in the **z** direction independently on its refractive index.
- The maximal force in the **z** direction occurs at the critical angle while the maximal attractive forces in the **y** direction occur for a slightly bigger angle. This is caused by the fact that the force F_y is generated purely by the gradient of the optical intensity in the liquid. As the angle of incidence increases, the gradient of the field also increases.

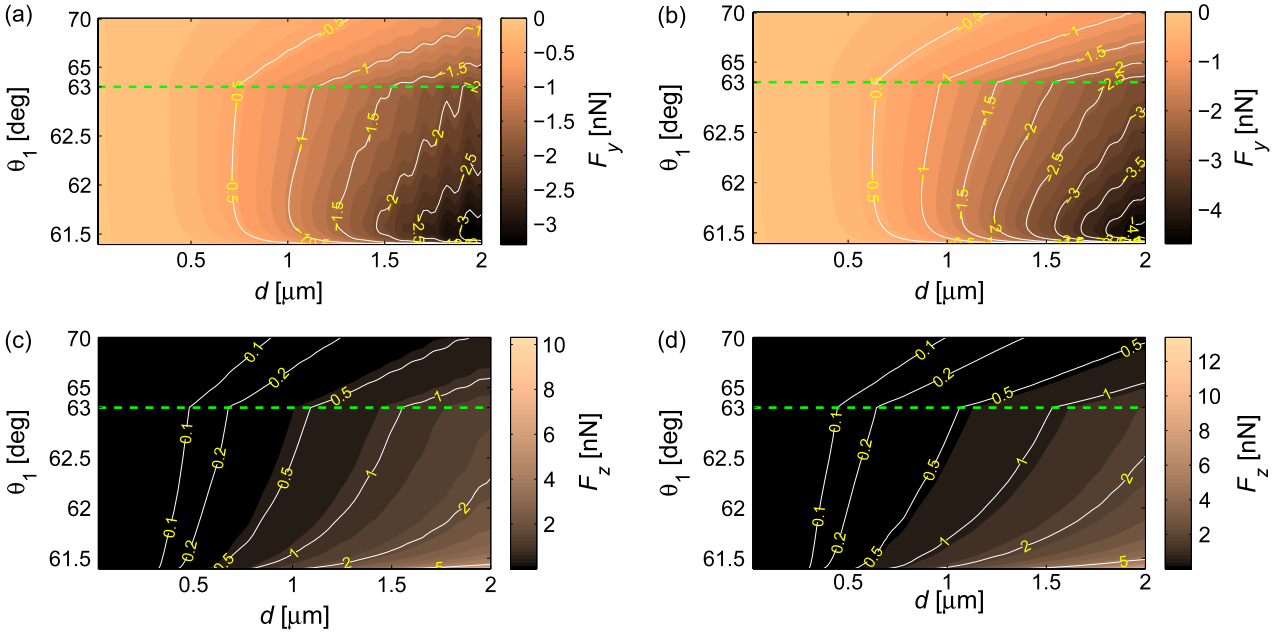

Figure 4. The forces acting upon a polystyrene particle of diameter d placed in water and illuminated by an evanescent field generated by a single plane wave with the incidence angle θ_1. The forces F_y act in the **y** direction ((a), (b)) and the forces F_z in the **z** direction ((c), (d)), respectively. The incident plane wave is either s-polarized ((a), (c)) or p-polarized ((b), (d)). The angles of incidence are differently scaled below and above the green dashed line denoting 63° to enhance the visibility of force changes near the critical angle.

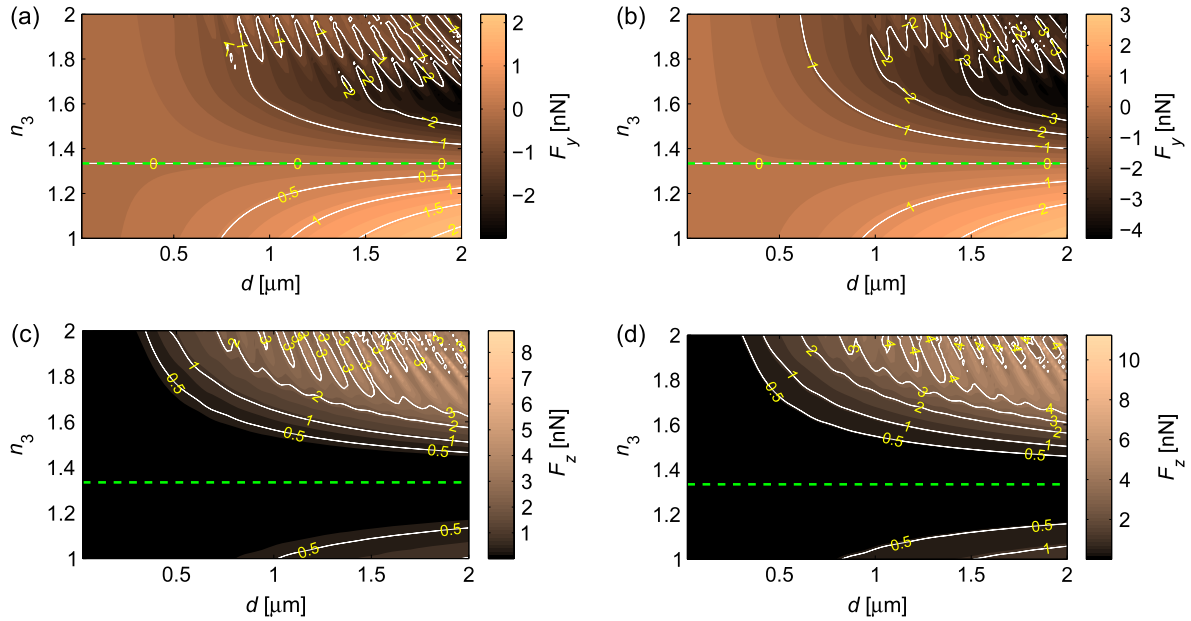

Figure 5. The forces acting upon a polystyrene particle of diameter d and refractive index n_3 placed in water and illuminated by an evanescent field generated by a single plane wave with the incidence angle $\theta_1 = 62°$. The meaning of the symbols is identical to figure 4.

However, the penetration depth of the field decreases and only a small part of the particle volume is influenced by the evanescent field. Therefore, after reaching the maximal attraction the force F_y tends to zero for higher angles of incidence. The force in the **z**-direction is of a purely scattering nature and, therefore, it only decreases with the increasing angle of incidence as does the affected the particle volume.

- Oscillations of the forces occur for larger particle diameters and refractive indices. These oscillations are connected to the so-called morphology dependent resonances (MDRs) [51] that occur if the denominators of the scattered wave expansion coefficients are close to zero [51, 52]. They were observed experimentally by Ashkin [53] more than 30 years ago in levitation experiments. For certain combinations of parameters these MDRs give a rise to so-called whispering gallery modes that lead to a huge enhancement of optical forces [54, 55]. The MDRs excited by an evanescent wave were theoretically studied by Jaising *et al* [27] considering a polystyrene particle placed in an evanescent wave leaking out of the slab optical waveguide. Using Mie theory and ignoring the interaction between the particle and waveguide interface they mentioned that the MDRs can lead to the repulsion of the particle from the slab waveguide interface even if the particle polarizability is positive. We used our model of a single EW illuminating the particle, applied the Mie model with ignored interaction between the particle and the interface, and we found only attractive force between the surface and the particle for similar parameters as Jaising *et al*. The reason of this disagreement could be different spatial distribution of the evanescent wave illuminating the particle near the waveguide comparing to the field assumed in this paper.
- The optical forces caused by the EW formed by a p-polarized incident plane wave are generally stronger than the forces caused by an s-polarized one. This is always true for F_y. However, the MDRs caused by both polarizations are slightly shifted for different particle diameters and, therefore, F_z^{s} can be stronger for certain particle refractive indices and diameters. figure 6 shows the ratio of forces $F_z^{\mathrm{s}}/F_z^{\mathrm{p}}$ and demonstrates the existence of regions with $F_z^{\mathrm{s}} > F_z^{\mathrm{p}}$.

4.2. *Two counter-propagating waves*

In this section we focus on two counter-propagating evanescent waves. We assume that both waves interfere and create a standing wave pattern at the prism–water interface. Furthermore, we assume that the electric field intensity of both waves is the same. Under these circumstances, the scattering force caused by the two waves is completely suppressed and only the gradient forces are present. We study here only the cases where both incident plane waves are either s- or p-polarized.

Since the scattering force is suppressed by the selection of the electric field intensities, the resulting optical forces are periodic and they have the same periodicity as the standing wave intensity. Therefore, the forces in the **y** and **z** directions can be generally expressed as follows

$$F_{y,z} = A_{y,z}\sin(2\gamma z + \Phi_{y,z}) + O_{y,z}, \qquad (12)$$

where A, Φ and O can be understood as the modulation amplitude, the phase shift at the coordinate origin, and the offset of the periodically modulated force along **y** and **z** axis, respectively. γ is the size of the wavevector along the prism boundary defined by equation (4). The values of A, Φ and O

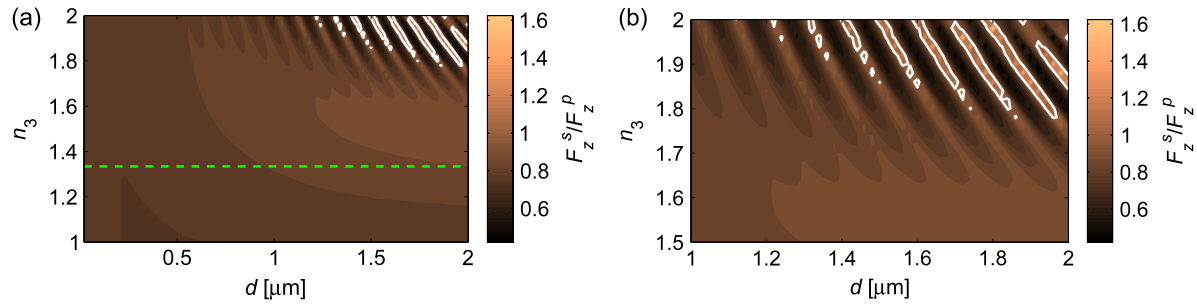

Figure 6. The ratio of forces F_z for s- and p-polarized incident plane waves shown in figures 5(c) and (d). The detail of the upper right quadrant of (a) is shown in (b). White contours denote $F_z^s/F_z^p = 1$.

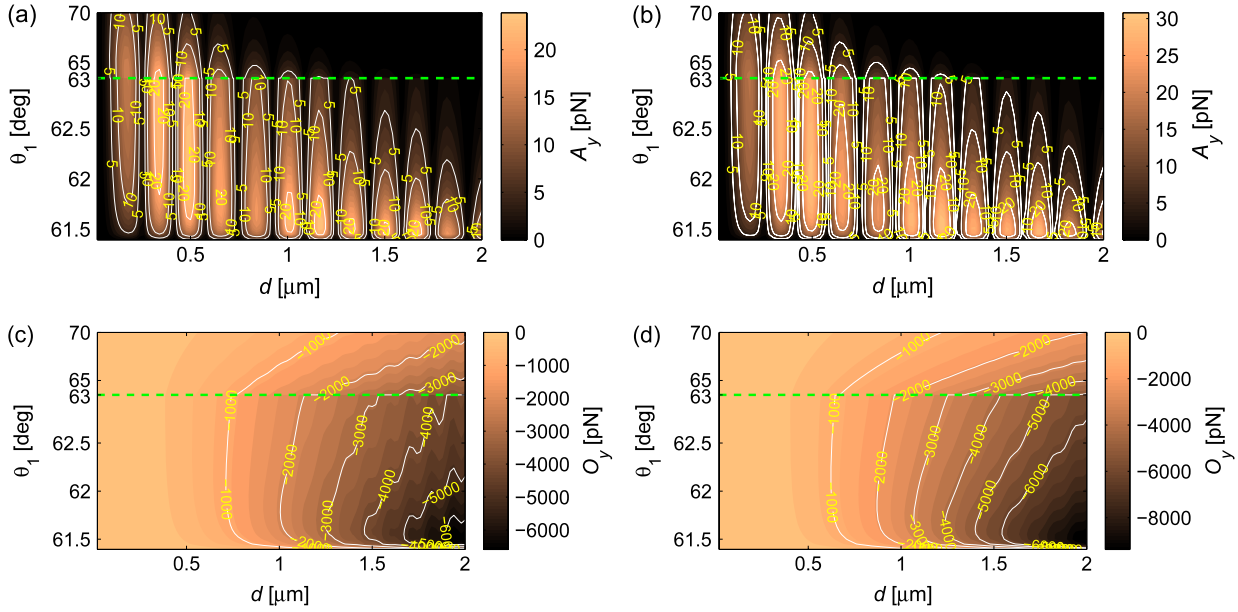

Figure 7. Amplitude A_y ((a), (b)) and offset O_y ((c), (d)) of force F_y acting upon the particle placed into the interference field of two counter-propagating evanescent waves. These waves are both formed by s- ((a), (c)) or p- ((b), (d)) polarized plane waves incident on the surface. The parameters of the calculations are the same as mentioned in the introduction.

are obtained by numerical calculations of optical forces using the MSM [16, 23].

Figures 7 and 8 show the results of parametric studies of the optical forces acting upon particles of different diameters illuminated by the evanescent standing wave. The forces are calculated at several points along the **z** axis and we use equation (12) to obtain amplitudes $A_{y,z}$, phase shifts $\Phi_{y,z}$, and offset O_y. figure 7 compares the amplitudes A_y and offsets O_y of the force F_y for s- and p-polarizations of the incident plane waves. The force modulation amplitudes for both polarizations are several orders of magnitude smaller than the overall force offsets. Therefore, the force F_y is negative for all z-coordinates (for the considered configuration of polystyrene particles immersed in water above the BK7 prism) and it pushes the particles to the surface. Similarly to the case of a single EW, the forces produced by p-polarized incident plane waves are stronger comparing to s-polarized ones.

Figure 8 shows the amplitude of the optical force in the **z** direction. Since the offset of this force component is $O_z = 0$, the sinusoidal modulation has zero points that are located $\lambda_{\mathrm{vac}}/(4n_1 \sin\theta_1)$ apart. Typically, the force F_z is smaller than the force in the **y** direction except the region very close to the critical angle where the force F_y is very small. Here, the forces in both **y** and **z** directions are of the same order. Furthermore, particles of certain diameters are very weakly influenced by the light field and they move almost freely between interference fringes while the particles of other diameters are confined to stable positions [56].

The phase shifts in the **z** direction Φ_z assume only two possible values, either 0 or π. The value of Φ_z determines which of the equilibrium positions of the force F_z would be stable or unstable. These values are connected to the standing wave fringes and it has been shown [56] that the particle settles with its centre either to the centre of the bright or dark fringe. This behaviour is independent of the polarization of the incident waves, i.e. the stable positions of the particle of a certain radius would be always either in the bright or dark fringes. Moreover, the particle's stable position is the same in the range of particle radii that are separated by the zero force

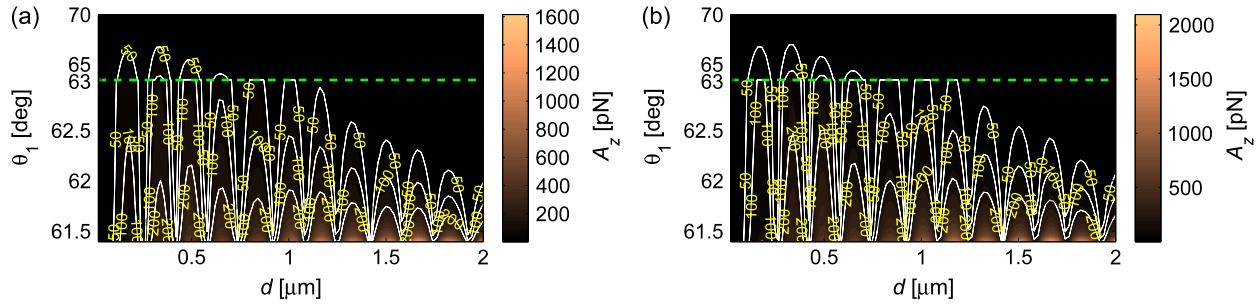

Figure 8. The amplitude A_z of the **z** component of the force acting on the particle placed into the interference field of two counter-propagating evanescent waves. The EWs are formed by s- (a) or p- (b) polarized plane waves incident on the surface. The parameters of the calculations are the same as in figure 7.

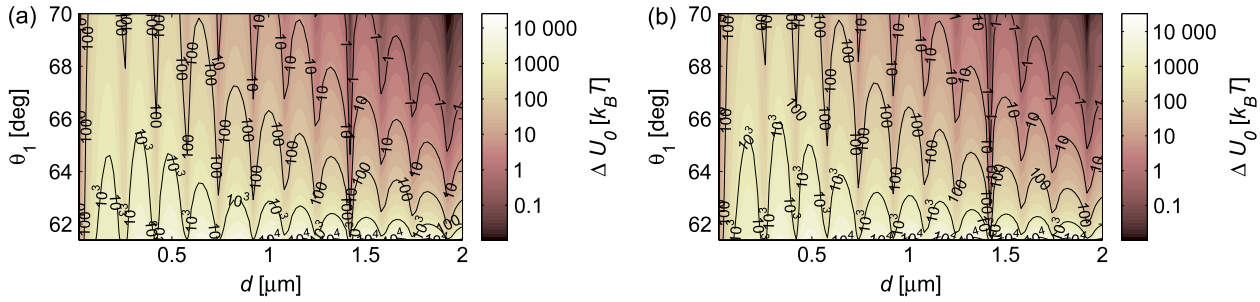

Figure 9. The trap depth ΔU_0 in the **z** direction. The incident plane waves are both either s- (a) or p- (b) polarized. The colour mapping in the figures is logarithmic, therefore, even the small trap depths near the angle of incidence 70° are visible.

amplitude, see figure 8. Furthermore, the shifts Φ_y in the **y** direction are connected to Φ_z so that the attractive force to the surface is maximal if the particle settles to its equilibrium position. The affinity of the particle to the interference pattern and the dependence of the particle equilibrium position on its size is called the 'size-effect'. It has been predicted and observed in interfering Gaussian beams [56–58], Bessel beams [59], and evanescent waves [14].

Since the non-conservative part of force F_z was eliminated by the choice of equal electric field intensities of counter-propagating waves, the potential energy U ($\mathbf{F} = -\nabla U$) can be defined using equation (12):

$$U(z) = -\frac{A_z}{2\gamma}\cos(2\gamma z+\Phi_z) = -\frac{\Delta U_0}{2}\cos(2\gamma z+\Phi_z), \quad (13)$$

where $\Delta U_0 = A_z/\gamma$ is the optical trap depth which corresponds to the height of the potential energy barrier between two neighbouring potential energy minima. Figure 9 shows the trap depth calculated from figure 8 in logarithmic colour mapping leading to better visibility of the details for bigger angles of incidence.

5. Conclusions

In this paper, we have studied the optical forces acting upon a spherical particle illuminated by an evanescent wave formed near the planar surface by incident plane waves. To calculate the optical forces we have used two methods ignoring the surface–particle interaction (Rayleigh approximation—RA—and Mie scattering—MSM) and two methods including the light reflections between the surface and the particle (Rayleigh approximation with the correction to the surface proximity—RASC—and finite element method—FEM). Using all the methods we have determined the optical force F_y acting perpendicularly to the surface and the force F_z acting parallel to the surface. In the case of the polystyrene particle of radius 5 nm immersed in water we have found very good agreement between F_y calculated by RA and MSM or RASC and FEM, respectively. For such a small particle the amplitudes of the F_z forces are smaller than F_y by three orders of magnitude and become comparable to the numerical errors during the FEM calculations. Therefore, the much smaller force F_z could not be expressed using FEM and RASC becomes the most effective method of optical force calculation for particles having a radius $a < \lambda/20$.

Considering the bigger particle of radius 50 nm, the force amplitudes along both directions are comparable and all forces can be expressed using FEM. Unfortunately, our desktop PC memory of 8 GB has not allowed us to study particles of radii bigger than $a \sim \lambda/4$ and separated more than $y_0 \sim \lambda/2$ from the surface.

While the calculations done by RA, RASC, as well as by MSM were almost instantaneous, the calculations performed by FEM took approximately 10 min for each particle–surface separation.

Our results show that MSM and FEM agree within 8% over the whole studied range of the particle–interface separations; for the particle–interface separations bigger than one particle radius, the agreement is better than 3%. Thus, MSM provides a very good first-order estimate of the optical

forces acting upon particles illuminated by evanescent fields in the vicinity of dielectric interfaces.

Based on the comparison of the FEM and MSM methods, we have applied MSM for a parametric study of the optical forces F_y and F_z acting upon polystyrene particles placed in water and illuminated by a single evanescent wave or a standing evanescent wave. We have considered different angles of incidence of the plane waves forming the evanescent waves, refractive indices of the particle, and particle diameters of up to 2 μm. In the majority of the studied configurations we have observed that p-polarized incident plane waves formed evanescent waves acting more strongly upon the particles in both the studied **y** and **z** directions. The exceptions were represented by rare cases of bigger and optically denser particles that have parameters close to the morphology dependent resonances for the used wavelength.

Acknowledgments

The authors appreciate the critical comments of Dr A Jonáš. This work was partially supported by the Institutional Research Plan of the Institute of Scientific Instruments (AV0Z20650511), the Ministry of Education, Youth, and Sports of the Czech Republic (projects No. LC06007, OC08034) together with the European Commission (project ALISI No. CZ.1.05/2.1.00/01.0017).

References

[1] Wazawa T and Ueda M 2005 Total internal reflection fluorescence microscopy in single molecule nanobioscience *Microscopy Techniques* (*Advances in Biochemical Engineering/Biotechnology* vol 95) ed J Rietdorf (Berlin: Springer) (http://www.springer.com/chemistry/biotechnology/book/978-3-540-23698-6)
[2] Hecht B, Sick B, Wild U, Deckert V, Zenobi R, Martin O and Pohl D 2000 *J. Chem. Phys.* **112** 7761–74
[3] Greffet J and Carminati R 1997 *Prog. Surf. Sci.* **56** 133–237
[4] Novotny L and Stranick S 2006 *Annu. Rev. Phys. Chem.* **57** 303–31
[5] Kawata S and Sugiura T 1992 *Opt. Lett.* **17** 772–4
[6] Ashkin A, Dziedzic J M, Bjorkholm J E and Chu S 1986 *Opt. Lett.* **11** 288–90
[7] Ashkin A 1970 *Phys. Rev. Lett.* **24** 156–9
[8] Berns M W and Greulich K O (ed) 2007 *Laser Manipulation of Cells and Tissues* vol 82 *Methods in Cell Biology* (San Diego, CA: Academic)
[9] Andrews D (ed) 2008 *Structured Light and its Applications* (San Diego: Elsevier Academic Press)
[10] Ashkin A 2006 *Optical Trapping and Manipulation of Neutral Particles Using Lasers* (London: World Scientific)
[11] Lang M J and Block S M 2003 *Am. J. Phys.* **71** 201–15
[12] Jonáš A and Zemánek P 2008 *Electophoresis* **29** 4813–51
[13] Oetama R J and Walz J Y 2002 *Colloid Surf.* A **211** 179–95
[14] Čižmár T, Šiler M, Šerý M, Zemánek P, Garcés-Chávez V and Dholakia K 2006 *Phys. Rev.* B **74** 035105
[15] Garcés-Chávez V, Dholakia K and Spalding G C 2005 *Appl. Phys. Lett.* **86** 031106
[16] Šiler M, Čižmár T, Šerý M and Zemánek P 2006 *Appl. Phys.* B **84** 157–65
[17] Yu X, Torisawa T and Umeda N 2007 *Chin. Phys. Lett.* **24** 2833–5
[18] Mellor C D and Bain C D 2006 *Chem. Phys. Chem.* **7** 329–32
[19] Reece P J, Wright E M and Dholakia K 2007 *Phys. Rev. Lett.* **98** 203902
[20] Girard C 2000 *Rep. Prog. Phys.* **63** 893–938
[21] Novotny L and Hecht B 2006 *Principles of Nano-Optics* (Cambridge: Cambridge University Press)
[22] Chang S, Jo J and Lee S 1994 *Opt. Commun.* **108** 133–43
[23] Almaas E and Brevik I 1995 *J. Opt. Soc. Am.* B **12** 2429–38
[24] Walz J 1999 *Appl. Opt.* **38** 5319–30
[25] Chaumet P, Rahmani A and Nieto-Vesperinas M 2002 *Phys. Rev. Lett.* **88** 123601
[26] Brevik I, Sivertsen T and Almaas E 2003 *J. Opt. Soc. Am.* B **20** 1739–49
[27] Jaising H Y and Hellesø O G 2005 *Opt. Commun.* **246** 373–83
[28] Kuriakose S, Gan X, Chon J and Gu M 2005 *J. Appl. Phys.* **97** 083103
[29] Lester M and Nieto-Vesperinas M 1999 *Opt. Lett.* **24** 936–8
[30] Ng L, Luf B, Zervas M and Wilkinson J 2000 *J. Lightw. Technol.* **18** 388–400
[31] Gaugiran S, Gétin S, Fedeli J M, Colas G, Fuchs A, Chatelain F and Dérouard J 2005 *Opt. Express* **13** 6956–63
[32] Gaugiran S, Getin S, Fedeli J M and Derouard J 2007 *Opt. Express* **15** 8146–56
[33] Šiler M and Zemánek P 2007 *Opt. Commun.* **275** 409–20
[34] Okamoto K and Kawata S 1999 *Phys. Rev. Lett.* **83** 4534–7
[35] Quidant R, Petrov D and Badenes G 2005 *Opt. Lett.* **30** 1009–11
[36] Novotny L, Bian R X and Xie X S 1997 *Phys. Rev. Lett.* **79** 645–8
[37] Song Y, Han B and Chang S 2001 *Opt. Commun.* **198** 7–19
[38] Chang S, Kim J T, Jo J H and Lee S S 1997 *Opt. Commun.* **139** 252–61
[39] Chaumet P C and Nieto-Vesperinas M 2000 *Phys. Rev.* B **61** 14119–27
[40] Nieto-Vesperinas N, Chaumet P C and Rahmani R 2004 *Phil. Trans. R. Soc. London* A **362** 719
[41] Ruiz-Cortés V and Vite-Frías J P 2008 *Opt. Express* **16** 6600–8
[42] Inami W and Kawata Y 2003 *J. Appl. Phys.* **94** 2183–7
[43] de Groot S R and Suttorp L G 1971 *Foundations of Electrodynamics* (Amsterdam: North-Holland)
[44] Chaumet P and Nieto-Vesperinas M 2000 *Opt. Lett.* **25** 1065–7
[45] Draine B 1988 *Astrophys. J.* **333** 848–72
[46] Barton J P, Alexander D R and Schaub S A 1989 *J. Appl. Phys.* **66** 4594–602
[47] Ren K, Gréhan G and Gouesbet G 1994 *Opt. Commun.* **108** 343–54
[48] Šiler M, Čižmár T, Jonáš A and Zemánek P 2008 *New. J. Phys.* **10** 113010
[49] Inami W and Kawata Y 2001 *J. Appl. Phys.* **89** 5876–80
[50] Robinson F N H 1975 *Phys. Rep.* **16** 313–54
[51] van de Hulst H C 1981 *Light Scattering by Small Particles* (New York: Dover) ISBN 0-486-64228-3
[52] Bohren C F and Huffman D R 1998 *Absorption and Scattering of Light by Small Particles* (New York: Wiley)
[53] Ashkin A and Dziedzic J 1977 *Phys. Rev. Lett.* **38** 1351–4
[54] Ng J, Chan C T, Sheng P and Lin Z 2005 *Opt. Lett.* **30** 1956–8
[55] Ng J and Chan C T 2008 *Appl. Phys. Lett.* **92** 251109
[56] Zemánek P, Jonáš A and Liška M 2002 *J. Opt. Soc. Am.* A **19** 1025–34
[57] Jákl P, Šerý M, Ježek J, Jonáš A, Liška M and Zemánek P 2003 *J. Mod. Opt.* **50** 1615–25
[58] Jákl P, Čižmár T, Šerý M and Zemánek P 2008 *Appl. Phys. Lett.* **92** 161110
[59] Čižmár T, Garcés-Chávez V, Dholakia K and Zemánek P 2005 *Appl. Phys. Lett.* **86** 174101